



BIOSYNTHESIS OF MAGNETITE-NANOPARTICLES USING MICROALGAE (*SPIRULINA* SP. AND *SPIROGYRA* SP.)

Hawar J. Sadiq Hawezy¹, Kwestan Hasan Sadiq², Vyan Asaad Qadr³, Sewgil Saaduldeen Anwer⁴
and Shameran Jamal Salih^{5*}

^{1,3,5}Department of Chemistry, Faculty of Science and Health, Koya University Park, Danielle Mitterrand Boulevard, Koya KOY45, Kurdistan Region of F.R. Iraq.

²Department of Medical Microbiology, College of Health Science, Hawler Medical University, Erbil-Kurdistan Region of F.R. Iraq

⁴Department of Clinical Biochemistry, Biotechnology College of Health Sciences, Hawler Medical University, Erbil-Kurdistan Region of F.R. Iraq.

Abstract

A promising avenue of research in materials science is to follow the strategies used by Mother-Nature to fabricate ornate hierarchical structures as exemplified by organisms such as diatoms, sponges and magnetotactic micro-algae. This paper focused on bio-synthesized magnetite nano-particles using eco-friendly method. Here, various microalgae have been used such as *Spirulina* sp. and *Spirogyra* sp. in order to produce magnetite nano-particles. The iron oxide nano-particles of average size~45 nm were obtained. Further, in this study different characterization technique's applied to obtain the magnetic nano-particles, scanning electron microscopy (SEM), energy dispersive X-Ray spectroscopy (EDX) and fourier-transform infrared spectroscopy (FT-IR). Also, X-ray diffraction, techniques. Calculation to obtaining the crystallite size by Debye-Scherrer equation. Also, The band gap parameters of the magneto-nanooxide such as indirect and direct-band gap energies has been determined ($E_g^{opt} = 1.87\text{eV}$ present study and $E_g^{opt} = 4.3\text{eV}$ elsewhere). Finally, the results of this paper clearly indicated that iron oxide-NPs spherical shaped and average size of particle is found to be below 100 nm.

Keyword : Biosynthesis; Magnetite nano-particles; Biofunctionalization; *Spyrogyra* sp. Surface grafting

Introduction

Nanotechnologies have been known to be used in numerous physical, biological and pharmaceutical applications. Synthesis of nanoparticles that have environmentally acceptable solvent systems and eco-friendly reducing agents is of great importance, such as in textile engineering, biotechnology and bioengineering, water treatment, electronics antibacterial/ antifungal agents in a diverse range of consumer products. *Spirulina* sp. and *Spirogyra* sp. are nonpathogenic microalgae that are wide word distributed and easy cultured under different growth condition. *Spirulina* is very high in(Ahmed *et al.*, 2015) protein, very low in calories and cholesterol, and high in enzymes, minerals (iron, calcium, sodium and magnesium), and phenolic acids, which have antioxidant properties.

Once materials are prepared in the form of very small particles, they change significantly their physical and chemical properties. In fact in nanodimension, percentage of surface molecule compare to bulk molecule is high and this enhances the activity of the particle in nano-dimension and therefore, the normal properties of the particle like heat treatment, mass transfer, catalytic activity, etc are all increases. But compare to non-metal nanoparticles, metal nanoparticles have more industrial application. Nanoparticles offer many new developments in the field of biosensors, biomedicine and bio nanotechnology-specifically in the areas- y Drug delivery y as medical diagnostic tools, y as a cancer treatment agent (gold nanoparticles) (Stancheva *et al.*, 2013). Nanoparticles and nanostructure are becoming a part in human medical application, including imaging or the delivery of therapeutic drugs to cell, tissues and organs. Drug loaded nanoparticles interact organ and tissues and are taken up by cells. Several studies have shown that the tissue, cell and even cell organelle distribution^{3,4} of drugs may be controlled and improved by their entrapment in colloidal

nanomaterials, mainly of the micellar structure, such as nano-container. Magnetic nanoparticles have been receiving considerable attention because of their wide range of applications, such as the immobilization of the proteins and enzymes, bio-separation, immunoassays, drug delivery, and biosensors. In general, the particle-size distribution in the magnetosome is narrow, whereas a broader-size range in some of the chemical synthesis grown crystals is common (Elblbesy, Madbouly and Hamdan, 2014). Finally, there are several important questions about magnetite synthesis that need to be addressed. Magnetic biogenic minerals are produced by microbial activity in a wide range of subsurface environments. Magnetite is usually produced by both Fe^{II} reducing and Fe^{II} oxidizing bacteria, and understanding the formation of biogenic magnetite is particularly important (Elblbesy, Madbouly and Hamdan, 2014) (Salih and Rashid, 2015). Here, we attempt to propose a new method for synthesis magnetic nano-particles from $\text{Fe}^{\text{II}}/\text{Fe}^{\text{III}}$ from ferrous salt using divers microalgae (*Spirulina* sp. and *Spirogyra* sp.).

Materials and Methods

Isolation and identification of microalgae

Cultures of microalgae were isolated from Gomaspan dam by spreading water samples collected in October from 5ml depth onto solid 2% agar medium (BG11) as described by (Yosef *et al.*, 2010) (Hebeish *et al.*, 2011). The cultures were incubated at 30°C and illuminated with day- light fluorescent tubes having 2200 lux using plant growth chamber, following the growth of colonies on the agar media. Pure microalgae removed with pasture micropipette, examined under light microscope and identified as described by (Rashid, Omar and Salih, 2016). After identification the pure colonies were gently blown into liquid medium then incubated at 30 °C and pH 8 to obtain biomass. After 14 days

incubation microalgae were harvested by centrifugation at 4000 rpm for 10 min. To determine cell dry weight the collected sample dried in oven at 70 °C 4-6hrs, and weighted quickly after drying as described by (El-Rafie *et al.*, 2011) (Salih, Anwer and Faraj, 2017). Furthermore, Iron oxide nanoparticles were synthesized by taking $\text{FeCl}_2 \cdot 4\text{H}_2\text{O}$ and $\text{FeCl}_3 \cdot 6\text{H}_2\text{O}$ (2:1 molar ratios) and were dissolved in 50 ml of de-ionized water in a 250ml conical flask and heated at 70°C with mild stirring using magnetic stirrer under atmospheric pressure. Then, after 20 minutes, 25 ml of the aqueous solutions of microalgae (*Spirulina* sp. and *Spirogyra* sp.) both has been used in different flasks, was added to the mixture, directly the light yellow color of the prepared microalgae turned to dark-brownish color. Also, After 20 min, 25 ml aqueous solution of NaOH was added to the mixtures with the rate of 2ml/min for allowing the iron oxide settle-down uniformly. Therefore, the mixture let to cool down at room temperature. Finally, the iron-oxide nanoparticles were collected by decantation to form magnetite nano-particles. Moreover, the magnetite formed were washed using deionized water then by ethanol and kept in dissector for later use.

Results and Discussions

After purification of microalgae, growing cells were observed under light microscope and photographed. Culture showed the following characters. The filaments were spiral, length (typically 100–150 microns) and with a diameter close to 7-9 microns identified as *Spirulina* sp. Trichomes Fig.1. It was identified according to (Elblbesy, Madbouly and Hamdan, 2014). Fig.2, shows filamentous that appear as green algae, helical or spiral arrangement of the chloroplasts, un-branched filaments and is one cell thick were identified as *Spirogyra* sp. This alga is characterized by the spiral ribbon-like chloroplasts in the cell. Pheravut and (Elblbesy, Madbouly and Hamdan, 2014), (Bruins, Kapil and Oehme, 2000) reported the morphological characteristics of each sample with cell dimensions (width and length), with the number and arrangement of chloroplast spirals/pyrenoids.

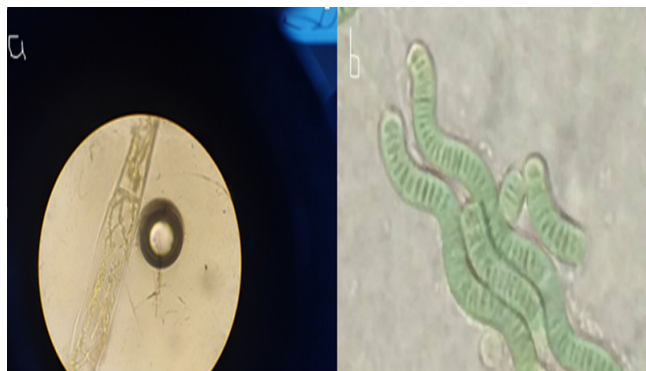


Fig. 1.a. : Light microscope and photographed of *Spirulina* sp. Trichomes and b. *Spirogyra* sp. that appear as green algae, helical or spiral arrangement of the chloroplasts, un-branched filaments and is one cell thick.

The mechanisms of magnetite formation by bacteria/microalgae are still under study and have been examined most intensively. The process by which the magnetosomes are made and organized is not completely known (Roh *et al.*, 2001). The comparison of the new method in preparation of magnetite with magnetite formation in magnetotactic bacteria is important. It shows how the magnetosomes are formed in bacterial bio-mineralization.

The crystalline size, morphology, and particle size distributions of synthetic magnetites compared to the magnetite isolated from magnetotactic bacteria are different. The magnetosome particle sizes typically are from 40 to 130 nm Fig. 2.

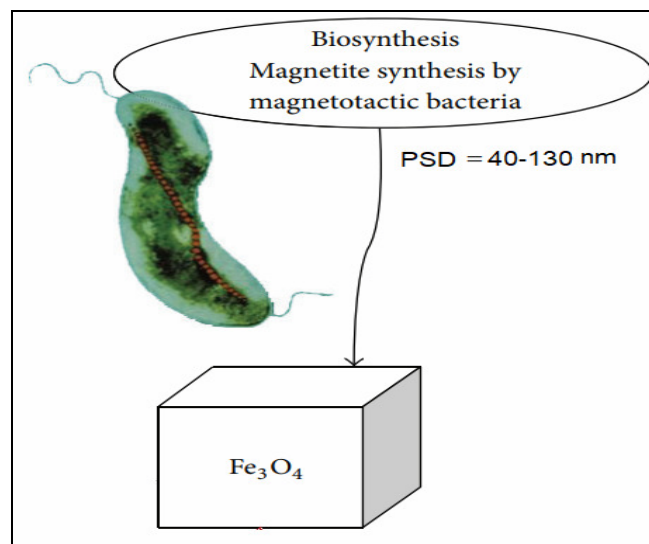


Fig. 2 : Proposed a schematic pathway of bio-synthesis of magnetite and their particles size distributions (Roh *et al.*, 2001)

Morphology Observation

The SEM image of the synthesized magnetite nanoparticles is shown in Fig. 3, 4 and 5. It is investigated that the magnetite nano-particles are agglomerated with the spherical-shape and narrow size distributions and grown in large-quantity with average-particle sizes of about 45 nm. However, the presence of agglomeration is clarified in terms of magnetic dipole-interactions between the nano-particles (Huang, Wang and Yan, 2010), (Leslie-Pelecky and Rieke, 1996), (Ahmed *et al.*, 2008). On the other hand, the typical EDS spectrum of the synthesis magnetite is observed in Fig. 5. It is good evidence that the synthesized magnetite is formed from $\text{Fe}^{\text{II}}/\text{Fe}^{\text{III}}$ and oxygen, only. The concentration of Fe is 57%, whereas oxygen is 29%. Except Fe and O, also some carbon detected peak that related with cell wall of the microbial in the spectrum (Nsar, Salih and Hawezy, 2019).

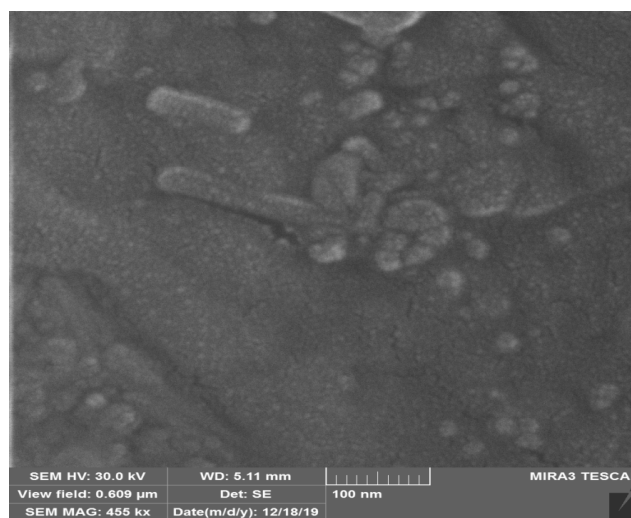


Fig. 3 : Field emission scanning electron microscope for narrow distribution of bio-synthesized nano-particles

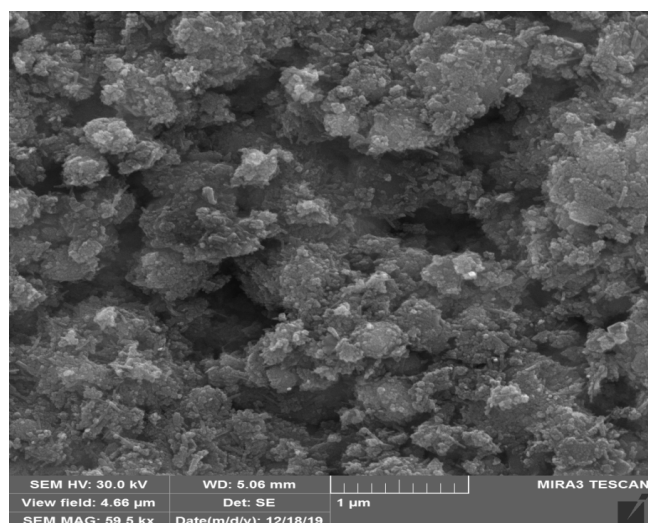


Fig. 4 : Field emission scanning electron microscope at different magnifications

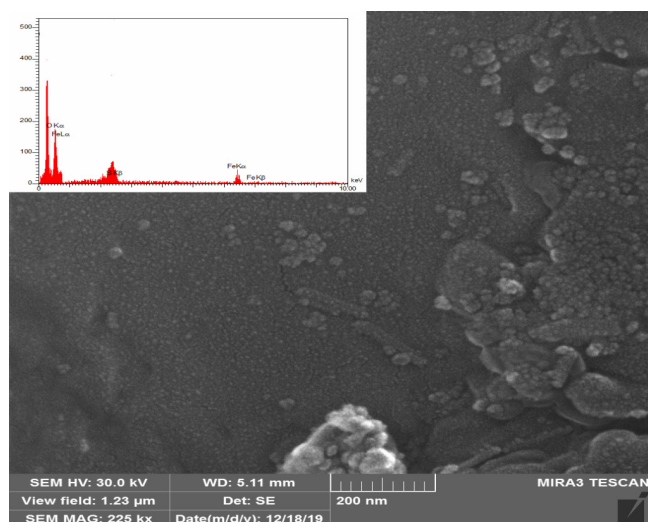


Fig. 5 : Field emission scanning electron microscope with EDX at different magnifications

FT-IR characterization

The FT-IR of pure *Spirulina* algae as shown in the Fig.6.a, where the vibrations at 3500-3560 cm^{-1} were attributed to the OH stretching of amino acids and carbohydrates additionally of the presence of alcohols and phenols (Salih and Faraj, 2017). In the range of 3500-3300 cm^{-1} the N-H stretching vibration of the secondary amines corresponded to the lipids and protein were noticed while from 3000 to 2850 cm^{-1} the aliquot C-H stretching vibration of the alkenes. Moreover, the frequency ranges 3300-2500 cm^{-1} represent the presence of the aliphatic OH stretching vibration of the carboxylic falls. With respect to the signals of 2260-2100 cm^{-1} was assigned to the triple bond C-C of the alkynes (Sulym *et al.*, 2016). The vibration of the carbonyl group C=O was located between 1750-1735 cm^{-1} . From 1680-1640 cm^{-1} corresponding to the stretching vibration of the C=C bond while the N-H flection of the ketone appeared between 1650-1580 cm^{-1} and the flection of the CH_2 group was showed between 1435-1405 cm^{-1} , respectively (Salih and Faraj, 2017) (Wu, Yuan and Fu, 2009). The range of 1550 to 1475 cm^{-1} was observed asymmetric stretching N-O corresponding to the nitrogenous compounds of the alga (Shameran, Sewgil and Awara, 2019).

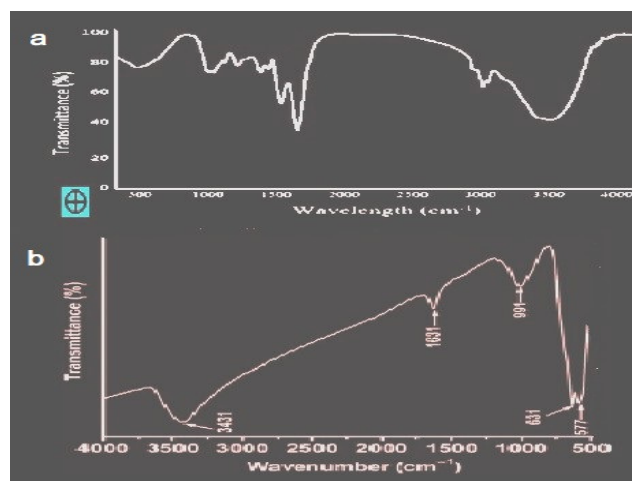


Fig. 6 : Spectrum of FTIR (a) the *Spirulina* sp. dried cell and (b) Iron oxide-MNPs synthesized

Fig. 6.b, clearly indicated that the iron oxide nanoparticles has been successfully biosynthesized, as the characterization of FT-IR showed that the exhibition of the typical spectrum of FT-IR which demonstrated divers well explained peaks at 577, 631, 991, 1631 and 3431 cm^{-1} . The presented of two peaks at 577 and 631 cm^{-1} are due to the presence of iron-oxygen FeO which indicated that the synthesized nanoparticles are iron-oxide (Salih and Hassan, 2017). In addition, the presented of a small peak at 991 is due to the appearance of NO_3 group. Furthermore, the peaks positioned at 1631 cm^{-1} and 3431 cm^{-1} are due to the absorbed vibration of H_2O and surface-hydroxyl and Hydroxide stretching mode, respectively.

Nevertheless, Spherical iron nanoparticles synthesized within biological microalgae (*Spirulina* sp.) acted as a catalyst for cross coupling reaction as shown in Fig. 7. Also, Bio-NPs have also been reported to synthesize directly on alginic acid and seaweed (*Laminaria digitata*, a brown alga with the common name Oarweed).

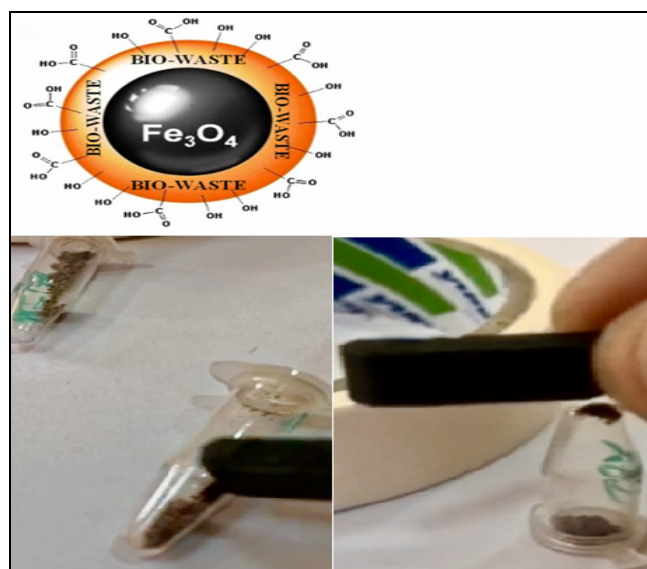


Fig. 7 : Biological synthesized of iron oxide-NPS and proposed surface of the Fe_3O_4 -NPs

Phase analysis

In order to characterized the phase identification and crystalline structures of the synthesized nanoparticles, x-ray

powder diffraction was used. The latter in one of the most significant usage of this technique. The x-ray diffraction (XRD) was conducted using x-ray diffractometer (Sulym *et al.*, 2016). Fig 8 shows XRD-spectra of biosyn-Fe₃O₄ and the particle size of the synthesized nano-oxide was determined using Debye-Scherrer equation according to;

$$L = \frac{K\lambda}{\beta \cos \theta} \quad \dots(1)$$

Additionally, the crystallite mean-diameter resulted from the diffractogram by using the above formula is 45 nm, which confirms the size observed by the electron micrographs above. Finally, the high intensity of these peaks confirmed strong scattering of the X-ray in the crystalline phase

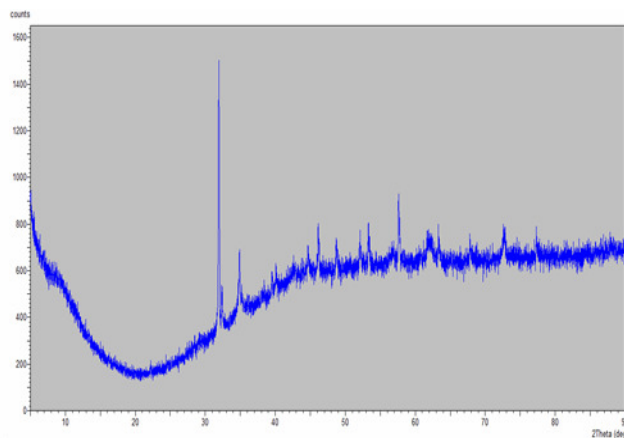


Fig. 8 : XRD-patterns of the magnetite nano-oxide

Spectroscopy measurement of Biosyn-Fe₃O₄

Fig. 9 shows the optical absorption (A) of Biosyn-Fe₃O₄ which is measured in a scanning range of wavelength from 190 to 1000 nm, with scan interval of 0.2 nm. On the other hand, the optical absorption obtained, it is possible to determine each of optical energy band gaps of indirect and direct transition occurring in band gap, Urbach energy and Fermi energy as following:

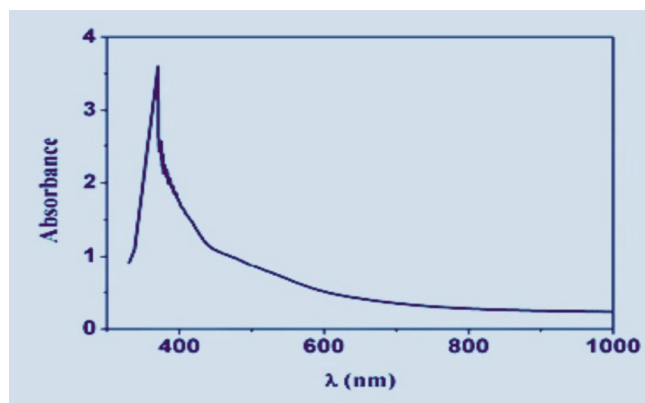


Fig. 9 : Absorbance Vs wavelength

Designation of band gap (Indirect and Direct transition) of iron-oxide NPs

Davis and Mott, gave an expression for the absorption coefficient, $\alpha(\nu)$, as a function of photon energy ($h\nu$) for indirect and direct transition through the following Eq.

$$A = -\ln\left(\frac{I}{I_0}\right) = \alpha(\nu)L \quad \dots(2)$$

$$\alpha(\nu) = \frac{A}{L} \quad \dots(3)$$

$$\alpha(\nu) = \frac{\alpha_0(h\nu - E_g^{opt})^n}{h\nu} \quad \dots(4)$$

where A is the absorption, I is intensity of transmitted light, I₀ is intensity of incident light, $\alpha(\nu)$ is the absorption coefficient of the sample, L is the thickness of the cell, α_0 is constant related to the extent of the band tailing, opt E_g is optical band gap energy and the exponent, n=2 for allowed indirect transition. In addition, by plotting $(h\nu\alpha)^{1/2}$ and $(h\nu\alpha)^2$ as a function of photon energy ($h\nu$), the optical energy band gap for indirect opt E_{g2} transition can be determined. Consequently, the respective values of opt E_g are obtained by extrapolating to $(h\nu\alpha)^{1/2}=0$ for indirect transition as shown in Fig. 10.

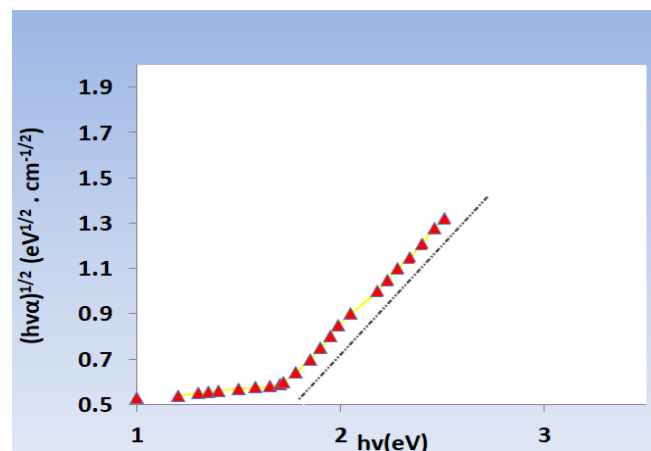


Fig. 10 : Indirect optical energy-band gap

Furthermore, the B_g energy of the NPs are inversely proportioned to its size. By this evidence, it is quite easy to say that the bandgap energy of NPs can be controlled by controlling their sizes. On the base of the value of indirect energy bandgap for the magnetite sample are classified this sample as a semiconductor, semiconductor energy band gap (0 - 3 eV) (Salih and Smail, 2016).

Conclusion

It is reasonable to say that the concern to magnetite-NPs with magnetic properties rapidly developed every year. These materials have found their characterization and their applications in medicine for treatment and diagnostics of serious diseases, where treatment by other methods is more durable and expensive. Moreover, synthesis of such nanomaterials with stable properties is not completely elaborated, since besides the size-factor, the character of their building micro-geometry, methods of identification and functional properties must be examined. Additionally, special attention should be paid to topography, biocompatibility of initial nanoparticles and sizes. On the other hand, just these parameters eventually determine the functional properties. In accordance with results of this work it's clearly shown that identification of synthesized nanoparticles can be realized most effectively by the change of their magnetic properties.

This is possible both, at the stage of their synthesis and after bio-functionalization.

References

- Ahmed, A.I. *et al.* (2008). 'Structural characterization of sulfated zirconia and their catalytic activity in dehydration of ethanol', *Colloids and Surfaces A: Physicochemical and Engineering Aspects*, Elsevier, 317(1–3): 62–70.
- Ahmed, E.A. *et al.* (2015). Biosynthesis of silver nanoparticles by *Spirulina platensis* and *Nostoc* sp, *Glo Adv Res J Microbiol*, 4(4): 36–49.
- Bruins, M. R., Kapil, S. and Oehme, F.W. (2000). 'Microbial resistance to metals in the environment', *Ecotoxicology and environmental safety*, Elsevier, 45(3): 198–207.
- El-Rafie, M.H. *et al.* (2011) 'Environmental synthesis of silver nanoparticles using hydroxypropyl starch and their characterization', *Carbohydrate Polymers*. Elsevier, 86(2): 630–635.
- Elblbesy, M.A.-A.; Madbouly, A.K. and Hamdan, T.A.-A. (2014). 'Bio-synthesis of magnetite nanoparticles by bacteria', *Am J Nano Res Appl.*, 2(5): 98–103.
- Hebeish, A. *et al.* (2011). 'Highly effective antibacterial textiles containing green synthesized silver nanoparticles', *Carbohydrate Polymers*. Elsevier, 86(2): 936–940.
- Huang, Y.-F.; Wang, Y.-F. and Yan, X.-P. (2010). Amine-functionalized magnetic nanoparticles for rapid capture and removal of bacterial pathogens, *Environmental science & technology*. ACS Publications, 44(20): 7908–7913.
- Leslie-Pelecky, D.L. and Rieke, R.D. (1996). 'Magnetic properties of nanostructured materials', *Chemistry of materials*. ACS Publications, 8(8): 1770–1783.
- Nsar, S.O.; Salih, S.J. and Hawezy, H.J.S. (2019). Adsorptive Behavior of Medicinal Product Based Activated Carbon for Removal of Pharmaceutical Active Compounds in Aqueous Phase. *Redlich-Peterson Studies*, Oriental Journal of Chemistry. Oriental Scientific Publishing Company, 35(2): 813.
- Rashid, B.Z.; Omar, R.A. and Salih, S.J. (2016). Characterization and antimicrobial efficiency of silver nanoparticles based reduction method, *International Journal of Current Microbiology and Applied Sciences*, 5(8): 802–810.
- Roh, Y. *et al.* (2001). Microbial synthesis and the characterization of metal-substituted magnetites, *Solid State Communications*. Elsevier, 118(10): 529–534.
- Salih, S.J.; Anwer, S.S. and Faraj, R.H. (2017). A biosorption of Mercury from wastewater using isolated *Aspergillus* sp. Modified 1, 10-Phenanthroline: Hill isotherm model, *Science Journal of University of Zakho*, 5(4): 288–295.
- Salih, S.J. and Faraj, R.H. (2017). Potential of Pistachio-Hard Shell Based Thiosemicarbazone-Acetophenone for Pb²⁺ Metal Sorption: Kinetic Studies, Isotherms Modeling and Optimization.
- Salih, S.J. and Hassan, R. (2017). Potential of Pistachio Thiosemicarbazone Sorption: Kinetic Studies, Optimization.
- Salih, S.J. and Rashid, B.Z. (2015). Cranberry Stem as an Efficient Adsorbent and Eco-Friendly for Removal of Toxic Dyes from Industrial Wastewater, *Physico Studies, International Journal of Pharmaceutical Chemistry*, 5(6): 207–217.
- Salih, S. J. and Smail, A.K. (2016). Synthesis, characterization and evaluation of antibacterial efficacy of zinc oxide nanoparticles, *Pharmaceutical and biological evaluations*, 3(3): 327–333.
- Shameran, J.S.; Sewgil, S.A. and Awara, K.S. (2019). Biosynthesis of Silver Nanoparticles Extracted Using *Proteus*. Sumy State University.
- Stancheva, R. *et al.* (2013). Identity and phylogenetic placement of *Spirogyra* species (Zygnematophyceae, Charophyta) from California streams and elsewhere¹, *Journal of phycology*. Wiley Online Library, 49(3): 588–607.
- Sulym, I. *et al.* (2016). Silica-supported titania–zirconia nanocomposites: structural and morphological characteristics in different media, *Nanoscale research letters*. SpringerOpen, 11(1): 111.
- Wu, B.; Yuan, R. and Fu, X. (2009). Structural characterization and photocatalytic activity of hollow binary ZrO₂/TiO₂ oxide fibers, *Journal of Solid State Chemistry*. Elsevier, 182(3): 560–565.
- Yosef, H.A.A. *et al.* (2010). Preparation and Reactions of Optically Active Cyanohydrins Derived from 4-Chlorobenzaldehyde, Cyclohexanone and 2-Methylcyclohexanone using the (R) Hydroxynitrile lyase from *Prunus amygdalus*, *Egypt. J. Chem*, 53(5): 745–775.